Evaluation of Images Depending on an Attenuation Correction in a Brain PET/CT Scan

Eun-Jin Choi[1], Mon-Taeg Jeong[2], Kyung-Rae Dong[3], Jong-Gil Kwak[1,4], Ji-Won Choi[5] and Jae-Kwang Ryu[6,*]

[1]*Department of Public Health and Medicine, Dongshin University Graduate School, 185, Geonjae-ro, Naju-si, Jeollanam-do 58245, Republic of Korea*
[2]*Department of Radiological Science, Dongshin University 185, Geonjae-ro, Naju-si, Jeollanam-do 58245, Republic of Korea*
[3]*Department of Radiological Technology, Gwangju Health University, 73, Bungmun-daero 419 beon-gil, Gwangsan-gu, Gwangju 62271, Republic of Korea*
[4]*Comprehensive Medical Examination Center, KS Hospital, 220, Wangbeodeul-ro, Gwangsan-gu, Gwangju 62248, Republic of Korea*
[5]*Department of Radiological Science, Jeonju University, 303, Cheonjam-ro, Wansan-gu, Jeonju-si, Jeollabuk-do 55069, Republic of Korea*
[6]*Depatment of Nuclear Medicine, Asan Medical Center, 88, Olympic-ro 43-gil, Songpa-gu, Seoul 05505, Republic of Korea*

Abstract - A Hoffman 3D Brain Phantom was used to evaluate two PET/CT scanners, BIO_40 and D_690, according to the radiation dose of CT (low, medium and high) at a fixed kilo-voltage-peak (kVp) with the tube current (mA) varied in 17~20 stages (Bio_40 PET/CT scanner: the tube voltage was fixed to 120 kVp, the effective tube current (mAs) was increased from 33 mAs to 190 mAs in 10 mAs increments, D_690 PET/CT scanner: the tube voltage was fixed to 140 kVp, tube current (mA) was increased from 10 mAs to 200 mAs in 10 mAs increments). After obtaining the PET image, an attenuation correction was conducted based on the attenuation map, which led to an analysis of the difference in the image. First, the ratio of white to gray matter for each scanner was examined by comparing the coefficient of variation (CV) depending on the average ratio. In addition, a blind test was carried out to evaluate the image. According to the study results, the BIO_40 and D_690 scanners showed a $<1\%$ change in CV value due to the tube current conversion. The change in the coefficients of white and gray matter showed that the Z value was negative for both scanners, indicating that the coefficient of gray matter was higher than that of white matter. Moreover, no difference was observed when the images were compared in a blind test.

Key words : Hoffman 3D brain phantom, Bio_40 PET/CT scanner, D_690 PET/CT scanner, Attenuation map

INTRODUCTION

Positron emission tomography-computed tomography (PET/CT), which has been developed recently, combines a PET scanner with an X-ray CT scanner. Therefore, PET/CT allows the convergence of anatomical and functional images in hardware, which provides the precise location of a lesion and improves the diagnostic performance of PET image itself (Bar-Shalom *et al*. 2003; Antoch *et al*. 2004). In

* Corresponding author: Jae-Kwang Ryu, Tel. +82-01-7341-3557, Fax. +82-2-3010-2308, E-mail. huhjoon11@naver.com

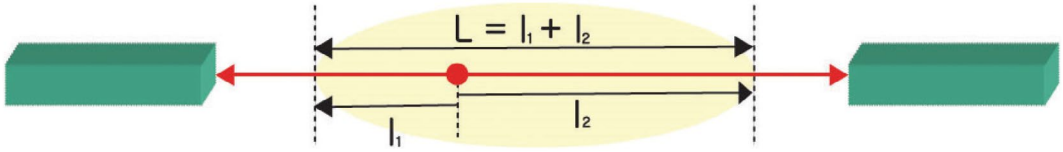

Fig. 1. Characteristics of the PET attenuation correction.

Blank scan Blank scan Emission scan

Fig. 2. Image for attenuation correction.

PET/CT, a CT image is not only conducive to a diagnosis but is also used as an attenuation map that is required for an attenuation correction in a PET emission scan. In a PET image, data correction is needed to improve the image quality. Data correction includes an attenuation correction, random coincidence correction, scatter coincidence correction, coefficient loss correction, and radioactivity attenuation correction. Among these corrections, the attenuation correction has the largest effect on the quality of PET images. The attenuation phenomenon in a PET image means that the degree of attenuation in the line of response (LOR) between two detectors is constant regardless of the location. If the respective values of the detection probability of the two gamma rays that are generated in a random point, as shown in Fig. 1, are multiplied by each other, the probability will be constant regardless of the location

$$E = E_0 \times \exp\left(-\int_0^{l_1} \mu(x,y)ds\right) \times \exp\left(-\int_0^{l_2} \mu(x,y)ds\right)$$
$$= E_0 \times \exp\left(-\int_0^{l_1+l_2=L} \mu(x,y)ds\right) \quad (1)$$

In addition, such a relation is equally valid between a blank scan (B) and transmission scan (T), as shown in eq. (2).

$$T = B \times \exp\left(-\int_0^{l_1+l_2=L} \mu(x,y)ds\right) \quad (2)$$

Therefore, emission scan data with the photon attenuation corrected can be acquired when a blank scan (B) and transmission scan (T) are divided for each pixel and multiplied by the emission scan data, as shown in eq. (3) (Fig. 2) (Cherry 2002; Chung and Lee 2008).

$$E_{0,\gamma\theta} = \frac{B_{\gamma\theta}}{T_{\gamma\theta}} \times E_{B_{\gamma\theta}} \quad (3)$$

The attenuation correction of a PET image using a CT image has some strong points compared to a transmission scan, which uses external sources (Kinahan *et al*. 1998; Von Schulthess 2000). First, the time to obtain a CT image is much shorter than in the case with a transmission scan, which enables a decrease in scan time. Second, a CT image has a much larger number of photons and higher resolution than a transmission image, which leads to much less noise in the attenuation map. For these reasons, it is important to perform a segmented attenuation correction (SAC), where the attenuation constants of some tissues are applied uniformly depending on the range of attenuation constants to reduce noise in a PET image obtained by a transmission scan using the external source and reduce the time needed for a transmis-

Fig. 3. Hoffman 3-D Brain Phantom.

sion scan. On the other hand, the measured attenuation correction (MAC) that uses a CT image enables the application of an attenuation constant in the form of a pixel unit that is obtained in an attenuation map but has a weak point of an increase in the patient's exposure to radiation (Xu *et al*. 1991; Bettinardi *et al*. 1999).

The difference in uptake of a PET image obtained using a CT image is a critical issue in the actual reading of a PET image. On the other hand, a CT scan is used only as a tool for an attenuation correction when the distribution of radiopharmaceutical is simply checked, as in the case with a brain PET/CT scan (such as dementia, epilepsy, Alzheimer's disease, etc.). Against this background, this study examined the effect of noise in an attenuation map on the attenuation correction when the CT dose is minimized as well as the baseline where no noise occurs.

MATERIALS AND METHODS

1. PET/CT system

This study was conducted using the PET/CT systems, Biograph Sensation 40 (SIEMENSE, German, hereafter BIO_40) and Discovery 690 (General Electric, USA, hereafter D_690). Both systems were reconstructed using an iterative reconstruction algorithm.

2. Image acquisition

^{18}F-FDG in 1 mCi (37 MBq) was diluted in water, and poured into a Hoffman 3-D Brain Phantom (Fig. 3). The image was obtained after one hour had passed.

3. Image data acquisition in BIO_40

When the tube voltage was fixed to 120 kVp, the effective

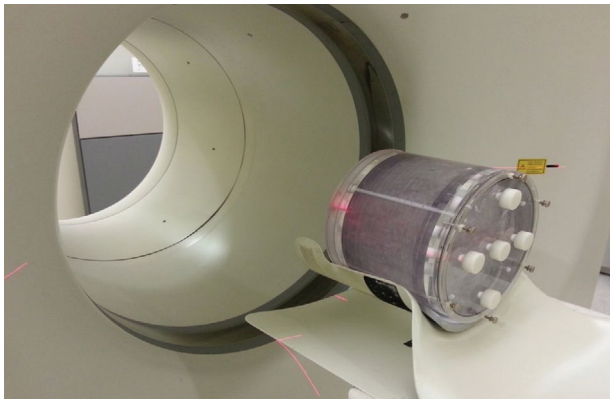

Fig. 4. Acquisition of the image data in BIO_40.

tube current (mAs) was increased from 33 mAs (minimum dose) to 190 mAs (maximum dose) in 10 mAs increments, and the Hoffman 3-D Brain Phantom was imaged (Fig. 4). A PET image (15 min/1 bed) was then obtained to draw and apply a correction to an attenuation map depending on each condition. In general, the degree of attenuation that occurs as the photon penetrates through the matter can be expressed as eq. (4).

$$\Phi = \Phi_0 \left[- \int_s \mu(x,y) dr \right] \quad (4)$$

where Φ and Φ_0 are the transmitted and incident photons per unit area, dr represents thickness of the medium, and μ represents the attenuation coefficient, which means the degree of the physical phenomena, such as the photoelectric effect or Compton scattering effect, as a photon passes through a medium in unit length.

The equation above was rearranged to derive eq. (5). In this case, $\exp[\int \mu(x,y)dr]$ is defined as the attenuation correction factor (ACF). The attenuation correction of the PET data involves multiplying the emission data by the ACF.

$$\int \mu(x,y)dr = \log_e\left(\frac{\Phi_0}{\Phi}\right) \quad (5)$$

4. Image data acquisition in D_690

When the tube voltage was fixed to 140 kVp, tube current (mA) was increased from 10 mAs to 200 mAs in 10 mAs increments, and the Hoffman 3-D Brain Phantom was imaged (Fig. 5). Subsequently, a PET image (10 min/1 bed) was obtained to draw and apply a correction to the attenuation map depending on each condition.

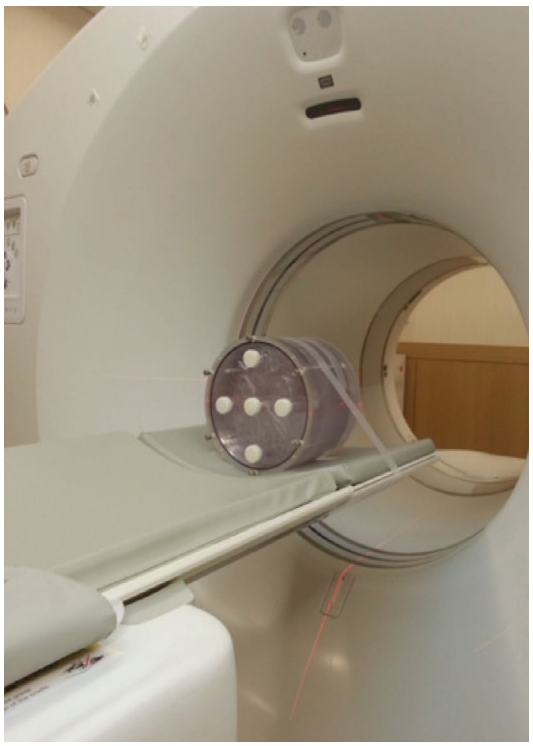

Fig. 5. Acquisition of the image data in D_690.

5. Coefficient variation depending on tube current variation

The PET raw data was used to create an attenuation-correction image based on the attenuation map that was drawn depending on each tube current using the CT image obtained from the Hoffman 3D Brain Phantom. The regions of interest (ROIs) for the white and gray matter were set to 0.5 square ×cm to calculate the coefficient of variation (CV) using each ratio in the same location (Fig. 6). In addition, the SPSS Version 15.0 program was used for statistical analysis. The mean minimum and maximum values were used to conduct a nonparametric Mann-Whitney U Test to examine the difference between the white and gray matter for each scanner. A p value <0.05 was considered significant.

6. Comparative analysis of image depending on tube current variation

The CT image obtained using the Hoffman 3D Brain Phantom was evaluated depending on the tube current variation by conducting a blind test on five nuclear medicine physicians working in a general hospital. In the ordinal scale, which was a qualitative scale, image resolution obtained with increasing tube current (mA) was scored as 5 points for "excellent," 4 points for "good," 3 points for "average," 2 points for "difficult to read," and 1 point for "unable to read." The scores were then averaged.

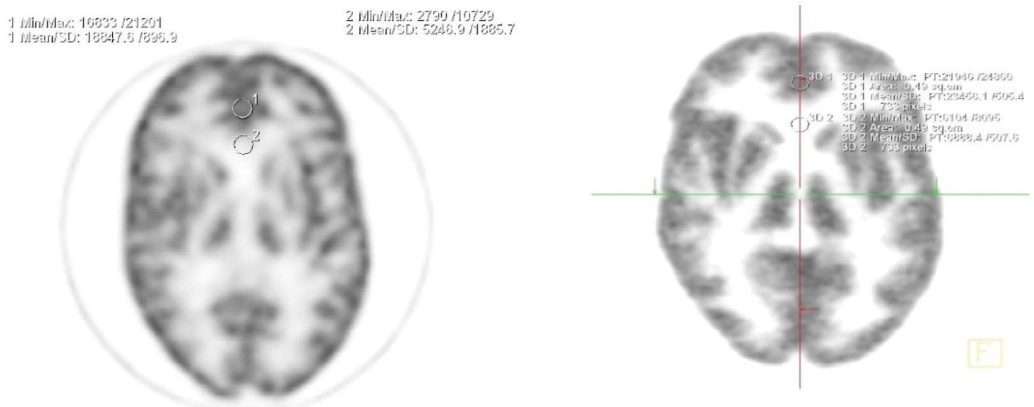

(a) BIO_40 (b) D_690

Fig. 6. ROI setting in BIO_40 (A) and D_690 (B).

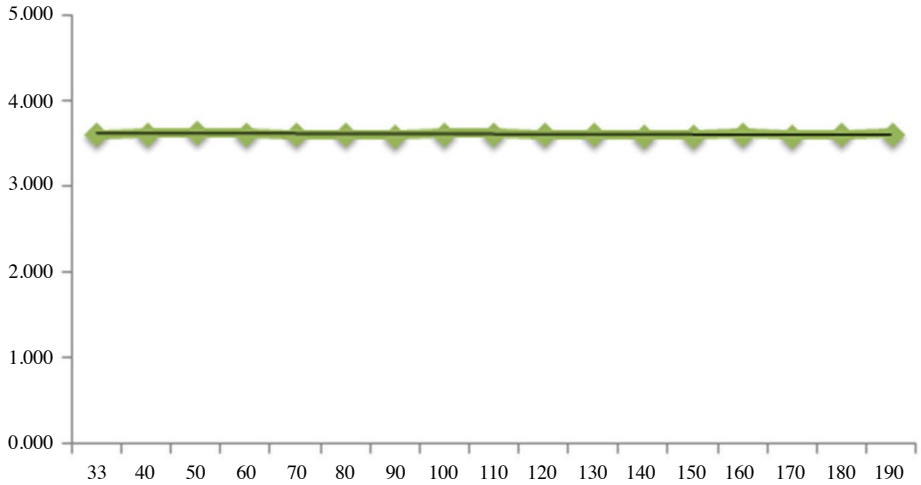

Fig. 7. Average ratio of the count number for the regions of interest of white and gray matter in BIO_40.

Table 1. Average ratio of the count for the regions of interest of white and gray matter in BIO_40

BIO_40	CT effective mAs	White matter			Gray matter			Average ratio
		Min	Max	Ave	Min	Max	Ave	
1	33	2777.0	10751.0	5247.2	17374.0	20759.0	18906.1	3.603
2	40	2696.0	10744.0	5232.5	17581.0	20437.0	18884.8	3.609
3	50	2786.0	10718.0	5243.4	16841.0	21193.0	18988.1	3.621
4	60	2782.0	10741.0	5246.3	16819.0	21262.0	18969.6	3.616
5	70	2786.0	10733.0	5243.7	16851.0	21196.0	18852.2	3.595
6	80	2496.0	10745.0	5254.0	16835.0	21217.0	18893.0	3.596
7	90	2790.0	10729.0	5246.9	16833.0	21201.0	18847.6	3.592
8	100	2510.0	10714.0	5216.9	16847.0	21215.0	18866.3	3.616
9	110	2790.0	10729.0	5246.9	16883.0	21201.0	18942.0	3.610
10	120	2788.0	10730.0	5248.6	17052.0	21201.0	18925.1	3.606
11	130	2786.0	10736.0	5252.5	17218.0	21202.0	18908.6	3.600
12	140	2787.0	10738.0	5248.0	16834.0	21199.0	18832.5	3.589
13	150	2787.0	10738.0	5248.9	16834.0	21199.0	18832.5	3.588
14	160	2780.0	10725.0	5243.1	16820.0	21180.0	18908.7	3.606
15	170	2783.0	10718.0	5239.0	16804.0	21186.0	18827.0	3.594
16	180	2786.0	10714.0	5244.9	16811.0	21172.0	18907.9	3.605
17	190	2781.0	10711.0	5235.2	16785.0	21149.0	18895.2	3.609
CV		0.034	0.001	0.002	0.013	0.010	0.003	0.003

RESULTS

1. Ratio of white matter to gray matter in BIO_40

In BIO_40, the average white to gray matter ratio was 3.603 at effective tube currents ranging from 33 mAs (the lowest dose) to 190 mAs (the highest dose). The CV for the average ratio was 0.003 (Table 1 and Fig. 7).

2. Ratio of white matter to gray matter in D_690

In D_690, the average white to gray matter ratio was 3.413 at tube currents ranging from 10 mAs (the lowest dose) to 200 mAs (the highest dose). The CV for the average ratio was 0.002 (Table 2 and Fig. 8).

3. Statistical analysis of white matter and gray matter in BIO_40 and D_690

The raw PET data was used to create an attenuation correction image based on the attenuation map that was drawn at each tube current using the CT image obtained from a Hoffman 3D Brain Phantom in BIO_40 and D_690 scanners. The ROIs for the white and gray matter were then set to 0.5 square × cm to conduct a non-parametric Mann-Whitney U

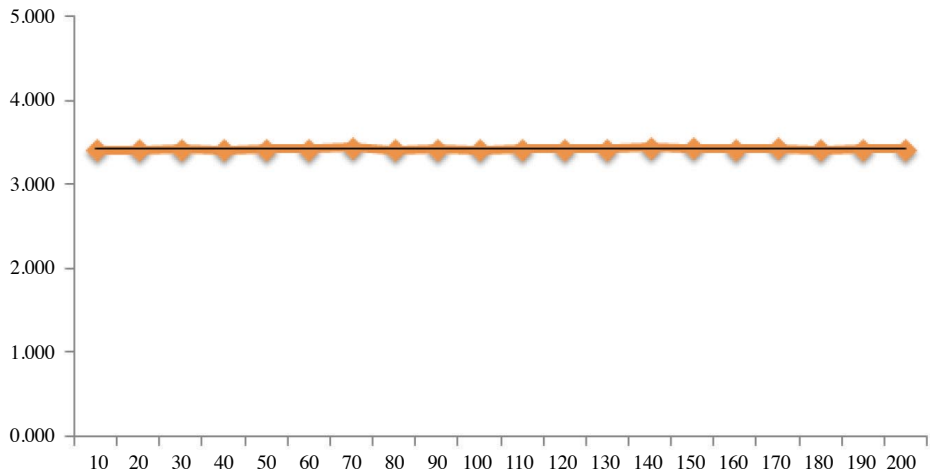

Fig. 8. Average ratio of the count number for the regions of interest of white and gray matter in D_690.

Table 2. Average ratio of the count for the regions of interest of white and gray matter in D_690

D_690	CT mA	White matter			Gray matter			Average ratio
		Min	Max	Ave	Min	Max	Ave	
1	10	6105	8201	6899	21838	24762	23510	3.408
2	20	6128	8193	6910	21893	24662	23533	3.406
3	30	5985	8101	6896	21967	25038	23530	3.412
4	40	6055	8110	6911	21899	24867	23532	3.405
5	50	6007	8111	6900	22032	24644	23523	3.409
6	60	6015	8114	6904	22035	24651	23602	3.419
7	70	5995	8099	6890	21994	24987	23632	3.430
8	80	5886	8032	6888	21946	25014	23456	3.405
9	90	5996	8082	6854	21962	25012	23383	3.412
10	100	5986	8105	6894	21943	24987	23475	3.405
11	110	6107	8166	6870	21986	24598	23432	3.411
12	120	6001	8094	6866	21999	24615	23419	3.411
13	130	6051	8104	6868	21990	24605	23423	3.410
14	140	5985	8063	6840	22205	24991	23470	3.431
15	150	5900	8047	6805	21966	25026	23297	3.424
16	160	5965	8050	6832	21987	25005	23325	3.414
17	170	5997	8075	6851	22103	25012	23473	3.426
18	180	6109	8164	6890	21819	24601	23469	3.406
19	190	6051	8112	6875	22051	24879	23470	3.414
20	200	6002	8054	6899	24693	22002	23523	3.410
CV		0.011	0.006	0.004	0.028	0.027	0.003	0.002

Table 3. Statistical comparison of the coefficients of white matter and gray matter in BIO_40 and D_690

Equipment	Region	N	Mean ± SD	Z	p
BIO_40	White matter of cerebrum	17	5243 ± 8.77	−4.978	0.000***
	Gray matter of cerebrum	17	18893 ± 47.04		
D_690	White matter of cerebrum	20	6677 ± 28.67	−5.412	0.000***
	Gray matter of cerebrum	20	23473 ± 81.76		

Note: Interaction effect using Mann-Whitney U Test. The unit is the number of count. ***$p < 0.001$

Test to compare the count in the same location. According to the analysis, the Z value of white matter from the BIO_40 and D_690 scanners was −4.978 and −5.412, respectively. These results show that the count for white matter was sig-

Table 4. Image comparison of BIO_40 depending on the change in tube current

BIO_40		
Effective mAs	N	Mean ± SD
33	5	5.00 ± 0.00
40	5	5.00 ± 0.00
50	5	5.00 ± 0.00
60	5	5.00 ± 0.00
70	5	5.00 ± 0.00
80	5	5.00 ± 0.00
90	5	5.00 ± 0.00
100	5	5.00 ± 0.00
110	5	5.00 ± 0.00
120	5	5.00 ± 0.00
130	5	5.00 ± 0.00
140	5	5.00 ± 0.00
150	5	5.00 ± 0.00
160	5	5.00 ± 0.00
170	5	5.00 ± 0.00
180	5	5.00 ± 0.00
190	5	5.00 ± 0.00

Table 5. Image comparison of D_690 depending on the change in tube current

D_690		
mA	N	Mean ± SD
10	5	5.00 ± 0.00
20	5	5.00 ± 0.00
30	5	5.00 ± 0.00
40	5	5.00 ± 0.00
50	5	5.00 ± 0.00
60	5	5.00 ± 0.00
70	5	5.00 ± 0.00
80	5	5.00 ± 0.00
90	5	5.00 ± 0.00
100	5	5.00 ± 0.00
110	5	5.00 ± 0.00
120	5	5.00 ± 0.00
130	5	5.00 ± 0.00
140	5	5.00 ± 0.00
150	5	5.00 ± 0.00
160	5	5.00 ± 0.00
170	5	5.00 ± 0.00
180	5	5.00 ± 0.00
190	5	5.00 ± 0.00
200	5	5.00 ± 0.00

nificantly lower than that for gray matter ($p < 0.05$) (Table 3).

4. Image comparison in BIO_40

When a blind test for BIO_40 was conducted to compare the attenuation correction image depending on the effective tube current (mA), the mean score was 5 points in all cases, showing similar images at the minimum and maximum doses (Table 4 and Fig. 9).

5. Image comparison in D_690

When a blind test conducted for D_690 to compare the attenuation correction image depending on the tube current (mA), the mean score was 5 points for all cases, showing similar images at the minimum and maximum doses (Table 5 and Fig. 10).

DISCUSSION

The recently developed PET/CT scanner has replaced the existing PET scanner owing to its many strong points. One of the differences between the existing PET image and PET/CT image is difference in the method of attenuation correction. PET is the representative image equipment that enables visualization of the body organs of interest in a functional and quantitative manner. In an existing PET image, an external source, such as ^{68}Ge and ^{137}Cs, is used to perform a transmission scan and conduct an attenuation correction. Since PET/CT was introduced, an attenuation correction was conducted based on the attenuation map, where the attenuation coefficient of the X rays for CT was converted to the attenuation coefficient of 511 keV photons for PET. For the attenuation correction, the γ rays emitted by the annihilation radiation from the human body have different intensities according to depth due to scattering and absorption. Therefore, to measure γ rays precisely, it is necessary to make a correction for the data that is obtained by actually measuring the data in advance for scattering and absorption by the human body. Such data collection for the purpose of correction is called a transmission scan. Scanning after injecting a radiopharmaceutical is called an emission scan. An absorption correction has the following strong points. The size, shape and location of a lesion can be described in a much more realistic manner. In addition, the radioactivity intensity of a lesion in body depth can be restored so that it is possible to measure the precise radioactivity concentration in the body and tumor. In PET, a transmission scan is performed as an external source that emits γ rays with similar energy to that of positron-emitting pharmaceutical with the body rotating once, as in the case of CT. The scan time is approximately 5∼15 minutes, which takes 10∼50% of the time for the entire examination. In the meantime, it takes a maximum of one minute in CT, even for a whole body scan. Therefore, the

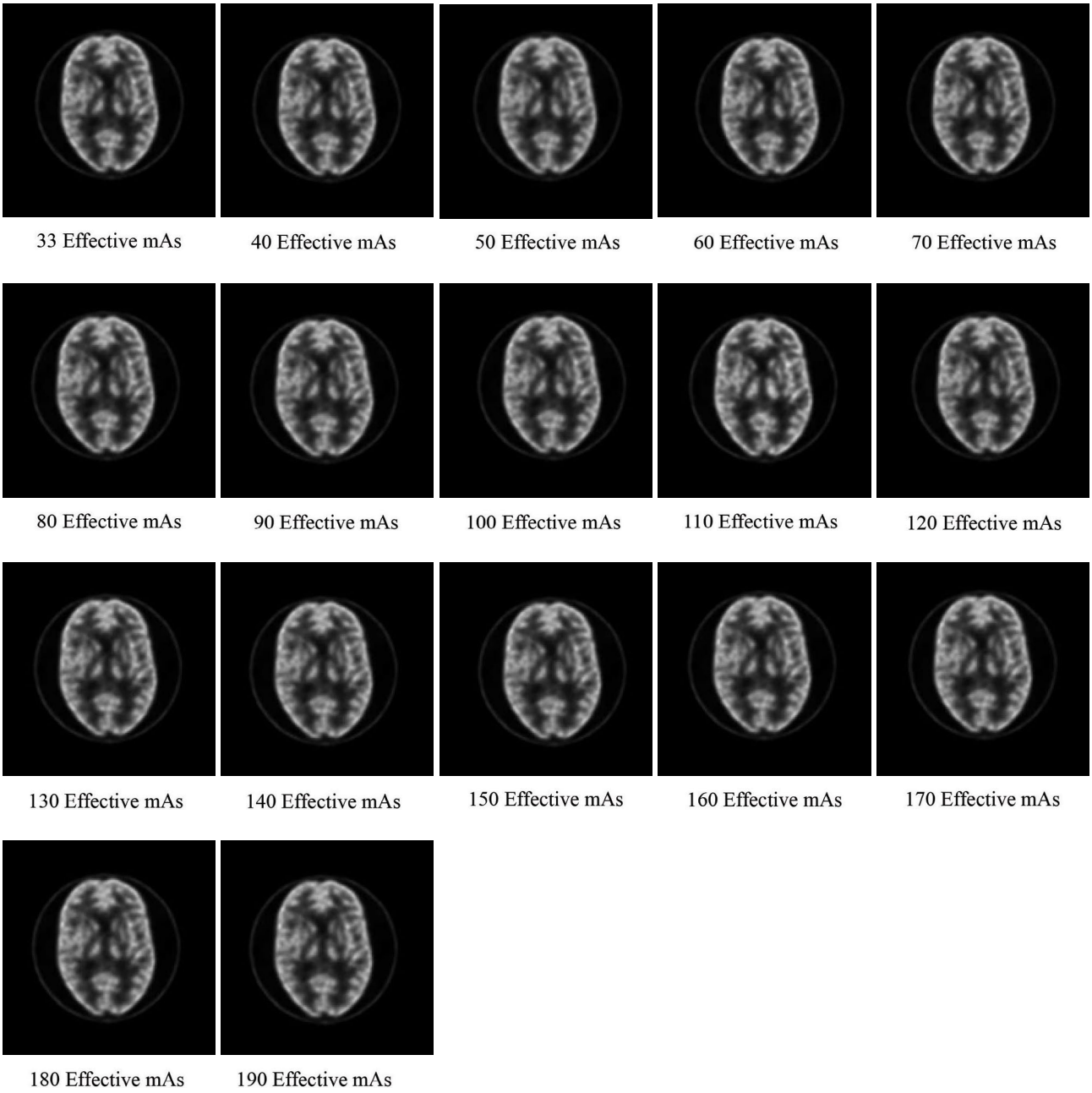

Fig. 9. Image comparison in BIO_40.

use of a CT-assisted attenuation correction (CTAC) would reduce the examination time by the amount of time required for the traditional transmission scan. CTAC can improve the PET image quality because the amount of data is sufficiently large compared to the case where an external source, such as ^{137}Cs or ^{68}Ge, is used. Therefore, an attenuation correction using CT can reduce the examination time, but it increases the patient's exposure dose. As a result, it was reported that a sufficient amount of data can be obtained when the tube current is reduced to 5 mA (Beyer *et al*. 2000; Son *et al*. 2005; Czernin *et al*. 2007; Kim *et al*. 2008). A Brain PET/CT scan requires a CT scout scan (topogram), which first uses CT to select the scan region, and a transmission scan, which is performed for attenuation correction. In this study, a Hoffman 3D Brain Phantom was examined using BIO_40 and D_690 PET/CT scanners. The dose for CT was classified as low dose (minimum dose), medium dose (normal dose for examination) and high dose (dose when a contrast agent is injected). With the tube voltage (kVp) fixed, the tube current (mA) was adjusted gradually in 17∼20 stages to obtain

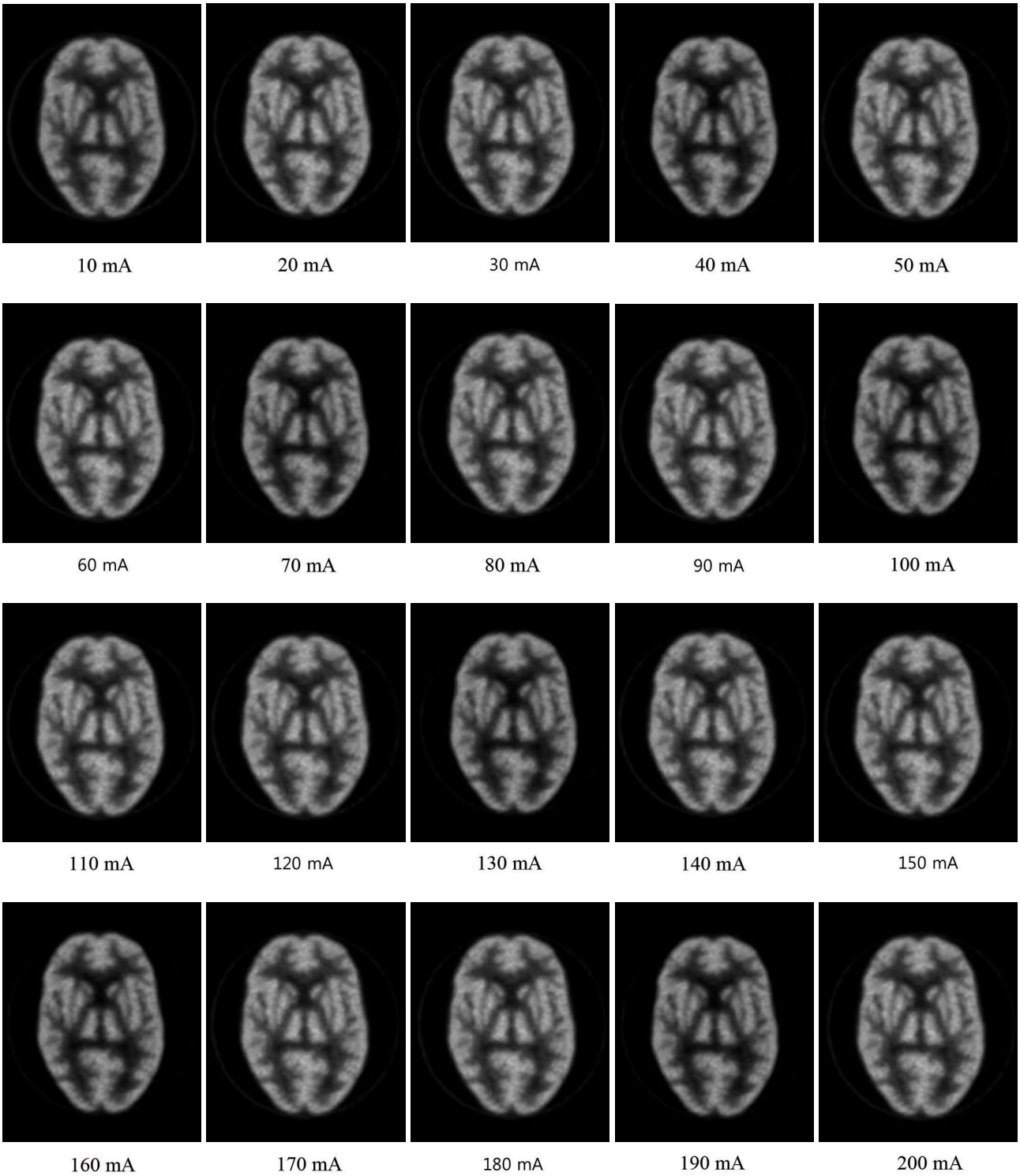

Fig. 10. Image comparison in D_690.

an image. After obtaining the PET image, an attention correction was made based on the attenuation map, which analyzes the difference in image according to the dose. The analysis results showed no difference in image quality. Consequently, this study confirmed that the difference in image quality was not significant in a CT scan used for an attenuation correction when the tube current (mA) is changed.

CONCLUSIONS

An attenuation correction is critical to improving the brain image quality. As the attenuation correction method can be conducted readily using CT, the use of low-dose CT for a transmission scan is expected to minimize the patient's exposure dose and improve image quality simultaneously in a brain examination conducted simply to examine the radiopharmaceutical distribution without the need to conduct a high image quality diagnostic CT scan.

REFERENCES

Antoch G, Saoud N, Kuehl H, Dahmen G, Mueller S, Beye T, Bockisch A, Debatin JF and Freudenberg LS. 2004. Accuracy of whole-body dual-modality fluorine-18-2-fluoro-2-deoxy-D-glucose positron emission tomography andcomputed tomography (FDG-PET/CT) for tumor staging in solid tumors: comparison with CT and PET. *J. Clin. Oncol.* **22**(21):4357-4368.

Bar-Shalom R, Yefremov N, Guralnik L, Gaitin D, Frenkel A, Kuten A, Altman H, Keidar Z and Lsrael O. 2003. Clinical performance of PET/CT in evaluation of cancer: additional value for diagnostic imaging and patient management. *J. Nucl. Med.* **44**(8):1200-1209.

Bettinardi V, Pagani E, Gilardi MC, Landoni C, Riddell C, Rizzo G, Castiqlioni I, Belluzzo D, Luciqnani G, Schubert S. and Fazio F. 1999. An automatic classification technique for attenuation correction in positron emission tomography. *Eur. J. Nucl. Med.* **26**(5):447-458.

Beyer T, Townsend DW, Brun T, Kinahan PE, Charron M, Roddy R, Jerin J, Young J, Byars L and Nutt RJ. 2000. A combined PET/CT scanner for clinical oncology. *Nucl. Med.* **41**(8):1369-1379.

Cherry SR, Sorenson JA and Phelps ME. 2002. Physics in Nuclear Medicine. 3rd ed. Saunders. Philadelphia.

Chung JK and Lee MC. 2008. Nuclear medicine. 3rd ed. Korea medicine. Seoul.

Czernin J, Allen-Auerbach M and Schelbert HR. 2007. Improvements in cancer staging with PET/CT: literature-based evidence as of September 2006. *J. Nucl. Med.* **48**(Suppl 1): 78S-88S.

Kim JS, Lee JS and Cheon GJ. 2008. Physical Artifact Correction in Nuclear Medicine Imaging: Normalization and Attenuation Correction. *Nucl. Med. Mol. Imaging* **42**(2):112-117.

Kinahan PE, Townsend DW, Beyer T and Sashin D. 1998. Attenuation correction for a combined 3D PET/CT scanner. *Med. Phys.* **25**(10):2046-2053.

Son HK, Turkington TG, Kwon YY, Jung HJ and Kim HJ. 2005. Impact of Contrast Agent for PET Images with CT-based Attenuation Correction. *Korean J. Med. Phys.* **16**(4):192-201.

Von Schulthess GK. 2000. Cost considerations regarding an integrated CT-PET system. *Eur. Radiol.* **10**(Suppl 3):S377-S380.

Xu EZ, Mullani NA, Gould KL and Anderson WL. 1991. A segmented attenuation correction for PET. *J. Nucl. Med.* **32**(1): 161-165.

Received: 26 July 2018
Revised: 17 August 2018
Revision accepted: 28 September 2018